GCM2-Activating Mutations in Familial Isolated Hyperparathyroidism

Bin Guan,[1,*] James M. Welch,[1] Julie C. Sapp,[2] Hua Ling,[3] Yulong Li,[1] Jennifer J. Johnston,[2] Electron Kebebew,[4] Leslie G. Biesecker,[2] William F. Simonds,[1] Stephen J. Marx,[1,5] and Sunita K. Agarwal[1,*]

Primary hyperparathyroidism (PHPT) is a common endocrine disease characterized by parathyroid hormone excess and hypercalcemia and caused by hypersecreting parathyroid glands. Familial PHPT occurs in an isolated nonsyndromal form, termed familial isolated hyperparathyroidism (FIHP), or as part of a syndrome, such as multiple endocrine neoplasia type 1 or hyperparathyroidism-jaw tumor syndrome. The specific genetic or other cause(s) of FIHP are unknown. We performed exome sequencing on germline DNA of eight index-case individuals from eight unrelated kindreds with FIHP. Selected rare variants were assessed for co-segregation in affected family members and screened for in an additional 32 kindreds with FIHP. In eight kindreds with FIHP, we identified three rare missense variants in *GCM2*, a gene encoding a transcription factor required for parathyroid development. Functional characterization of the *GCM2* variants and deletion analyses revealed a small C-terminal conserved inhibitory domain (CCID) in GCM2. Two of the three rare variants were recurrent, located in the GCM2 CCID, and found in seven of the 40 (18%) kindreds with FIHP. These two rare variants acted as gain-of-function mutations that increased the transcriptional activity of GCM2, suggesting that *GCM2* is a parathyroid proto-oncogene. Our results demonstrate that germline-activating mutations affecting the CCID of GCM2 can cause FIHP.

Introduction

Calcium is crucial for many physiological functions, including muscle contraction, secretion of neurotransmitters and hormones, blood coagulation, and mineralization of bone. Serum calcium homeostasis is maintained by an intricate balance between the amounts of calcium that are absorbed from the gut, exchanged with the bones, and excreted from the kidney. This balance is mainly controlled by parathyroid hormone (PTH), produced by the four parathyroid glands. PTH increases serum calcium levels by stimulating calcium release from bone, enhancing renal calcium reabsorption, and indirectly stimulating intestinal calcium absorption by increasing conversion of 25-hydroxy vitamin D to the active metabolite 1,25-dihydroxy vitamin D. In turn, the synthesis and secretion of PTH in the parathyroid glands is controlled by a feedback pathway, in which hypocalcemia stimulates PTH synthesis and secretion, whereas hypercalcemia inhibits these.

The parathyroid glands are susceptible to hyper-functioning due to parathyroid adenoma or hyperplasia. Primary hyperparathyroidism (PHPT), often caused by a single adenoma (80%–85%) or hyperplasia or adenomas involving multiple glands (15%–20%), is the major cause of hypercalcemia.[1] PHPT is common and occurs in individuals of all ages, but its prevalence is lower in young adults and increases with advancing age, with the highest prevalence in postmenopausal women.[1] The classical symptoms of PHPT include nephrolithiasis, osteoporosis, and neuromuscular symptoms associated with hypercalcemia, such as muscle weakness, drowsiness, and depression. With the inclusion of serum calcium measurement in the standard blood chemistry panels in the 1970s, and subsequent development of immunoassay for intact serum PTH, the majority of PHPT cases in many Western countries have become subtle or asymptomatic, with about 20% of individuals presenting with nephrolithiasis or osteoporosis.[2] In developing countries, the symptomatic forms of PHPT still dominate.[1]

Parathyroid tumors and PHPT can be caused by germline (hereditary PHPT) or somatic (sporadic PHPT) mutations of tumor suppressor genes (e.g., *MEN1* [MIM: 613733] and *CDC73* [MIM: 607393]) and proto-oncogenes (e.g., *RET* [MIM: 164761] and *CCND1* [MIM: 168461]). Approximately 5%–15% of PHPT cases occur in a familial setting, either in an isolated form (familial isolated hyperparathyroidism [FIHP]) or associated with other syndromal features—multiple endocrine neoplasia type 1 (MEN1 [MIM: 131100]), multiple endocrine neoplasia type 2A (MEN2A [MIM: 171400]), familial hypocalciuric hypercalcemia (FHH [MIM: 145980, 145981, and 600740]), neonatal severe hyperparathyroidism (NSHPT [MIM: 239200]), or hyperparathyroidism-jaw tumor syndrome (HPT-JT [MIM: 145001]) (Table S1).[3–8] The differential diagnosis can be assisted by clinical features. Individuals with a family history of PHPT but with no other non-parathyroid manifestation are provisionally diagnosed with FIHP. However, gene testing is the preferred diagnostic criterion because biochemical ranges can overlap among syndromes; specifically, PHPT diagnosed biochemically can be the first manifestation in individuals with MEN1, HPT-JT, or FHH

[1]The National Institute of Diabetes and Digestive and Kidney Diseases, Bethesda, MD 20892, USA; [2]The National Human Genome Research Institute, Bethesda, MD 20892, USA; [3]The Center for Inherited Disease Research, Johns Hopkins University, Baltimore, MD 21224, USA; [4]The National Cancer Institute, Bethesda, MD 20892, USA; [5]The Eunice Kennedy Shriver National Institute of Child Health and Human Development, Bethesda, MD 20892, USA
*Correspondence: bin.guan@nih.gov (B.G.), sunitaa@mail.nih.gov (S.K.A.)
http://dx.doi.org/10.1016/j.ajhg.2016.08.018.

syndromes. The post-DNA-test diagnosis of such FIHP cases can be changed to an occult form of the corresponding syndrome associated with the mutated gene.[6,9–11] Genetic testing might also identify a group of people with germline mutations but without apparent family history of PHPT.[6] This could be due to family members not having been investigated for PHPT or the proband having a de novo germline mutation, which could predispose children to PHPT. FIHP is inherited in an autosomal-dominant mode; however, specific mutations for or other causes of FIHP are unknown.

The lack of previous identification of a gene(s) associated with FIHP results from small family size, late age of diagnosis of hypercalcemia, lack of non-parathyroid traits to establish a separating diagnosis, and lack of a consensus region of loss of heterozygosity in tumors.[9] Furthermore, each of these features contributes to uncertainty as to whether a family with multiple affected individuals represents an inherited germline variant or a phenocopy. We evaluated 40 unrelated kindreds with FIHP and performed exome analyses in eight kindreds to identify genes potentially associated with FIHP.

Subjects and Methods

Subjects

Subjects were sampled and analyzed after giving written informed consent, according to protocols approved by the institutional review boards of the National Institute of Diabetes and Digestive and Kidney Diseases, the National Human Genome Research Institute, and the National Cancer Institute. Diagnosis of FIHP was made on the basis of previously described criteria.[9,11] Individuals were diagnosed with PHPT if they presented with hypercalcemia and elevated or unexpected normal circulating PTH. At least one family member with PHPT in each FIHP kindred had histopathologically verified abnormal parathyroid tissue. In total, we evaluated 40 apparently unrelated FIHP kindreds (37 with European ancestry, 2 with African ancestry, and 1 with mixed ancestry; Table S2). The proband plus at least one first-degree relative had PHPT in 36 of these 40 FIHP-affected kindreds. In the other four kindreds, the proband plus a second- or third-degree relative had PHPT. All but three probands or index cases were evaluated as inpatients at the NIH. None of the probands or index cases tested had germline mutations in *MEN1*, *CDC73*, or *CASR* (MIM: 601199), as determined by Sanger sequencing (GeneDx). *MEN1* and *CDC73* duplication and deletion tests were performed selectively (GeneDx). Eight index-case individuals of European ancestry from eight kindreds with FIHP who were available to give consent for exome sequencing at the time this study was initiated did so and constituted the exome cohort; the remaining 32 kindreds with FIHP served as the prevalence-screening (validation) cohort (Table S2).

A total of 87 pairs of matched blood and parathyroid tumor DNA samples were prepared from individuals diagnosed with sporadic PHPT (14 of African descent, 2 of East Asian descent, 32 of European descent, 11 of Latino descent, and 28 of unknown ancestries). Another set of 20 parathyroid tumor RNA samples from de-identified individuals with sporadic PHPT was previously processed into first strand cDNA. These 20 cDNA samples did not have matched germline DNA available.

Exome Sequencing and Analyses

Exome sequencing and bioinformatics pipelines were carried out as described in the ClinSeq project.[12] In brief, exome sequencing was performed on Illumina HiSeq instruments that gave sufficient coverage to allow 85% of the targeted exome to be called with high-quality variant detection (reported as genotype at every callable position). We aligned reads to the human reference genome (NCBI build 37 hg 19) with NovoAlign (Novocraft Technologies). We called genotypes by using only those sequence bases with Phred base qualities of at least Q20 by most probable genotype (MPG) and an MPG score of $\geq$ 10. ANNOVAR was used to annotate the variants with minor-allele frequencies (MAFs) from the ClinSeq study (938 subjects), the NHLBI GO Exome Sequencing Project ([ESP] 6,500 subjects), and the 1000 Genomes Project (1,092 subjects). Allele frequencies were also obtained from the Exome Aggregation Consortium (ExAC) database (release 0.3.1), containing data from 60,706 unrelated individuals. Rare variants with MAF $<$ 1% in ClinSeq, the NHLBI ESP, and 1000 Genomes were identified and prioritized for further analyses as detailed in the Results.

Sanger Sequencing

The majority of the PCR primers for Sanger sequencing were published oligos.[13] The M13 forward primer (5′-GTAAAACGACGGC CAGT) was appended to one of the primers in each primer pair and used for sequencing (Genewiz, single-pass sequencing in 96-well plate). The primer sequences for *GCM2* are listed in Table S3. The PCR reactions were carried out with 3–5 ng of genomic DNA in a 10 μL reaction as previously described, with minor modifications.[14] The PCR components were as follows: 1× PCR buffer (67 mM Tris-HCl [pH 8.8], 6.7 mM $MgCl_2$, 16.6 mM NH_4SO_4, 10 mM 2-mercaptoethanol), 1 mM dNTPs, 0.5 μM forward and 0.5 μM reverse primers, 6% DMSO, 2 mM ATP, and 0.06 μl Platinum Taq (Invitrogen). PCR cycling conditions were 95°C for 5 min; three cycles of 94°C for 15 s, 64°C for 20 s, and 70°C for 30 s; three cycles of 94°C for 15 s, 61°C for 20 s, and 70°C for 30 s; three cycles of 94°C for 15 s, 58°C for 20 s, and 70°C for 30 s; and 41 cycles of 94°C for 15 s, 57°C for 20 s, and 70°C for 35 s; followed by 70°C for 5 min. The Mutation Surveyor software v.4.0.9 (Softgenetics) was used for variant/mutation calling of the Sanger sequencing traces.

Plasmid DNA Constructs

Wild-type *GCM2* cDNA (GenBank: NM_004752.3) was PCR amplified from a human parathyroid cDNA sample and cloned into the pcDNA6-3xFLAG (lower case x) vector, yielding a N-terminal FLAG-tagged GCM2 expression construct. *GCM2* mutation constructs encoding p.Gly203Ser, p.Ile227Val, p.Tyr282Asp, p.Asn315Asp, p.Tyr394Ser, and the *cis* variant p.[Gln251Glu; Leu379Gln] (Table 1) were generated by PCR from the blood DNA from corresponding individuals and cloned into the EcoRI and XhoI sites of the wild-type *GCM2* construct. The p.Gln251Glu and p.Leu379Gln single variants were made by swapping the wild-type with the p.[Gln251Glu; Leu379Gln] *cis* variant region through subcloning (KpnI sites). The *GCM2* p.Val382Met[15] and deletion constructs were prepared by a PCR-ligation-PCR method, as previously described.[16] All of the *GCM2* expression constructs were made on the same backbone and contain the 3xFLAG tag.

Table 1. *GCM2* Variants in Cases of Hyperparathyroidism

DNA[a]	Protein	FIHP-Affected Kindreds[b]	Co-segregation Test	Trans-activating Activity[c]	ExAC Allele Frequency[d]							
					All	African	East Asian	European (Non-Finnish)	Finnish	Latino	South Asian	Other
c.−44T>C	5′ UTR	213, 715, 793	n.d.	n.d.	0.1032	0.4172	0.0532	0.0735	0.0886	0.1719	0.0314	0.1042
c.462G>A	p.Lys154 =	130 (African)	n.d.	n.d.	0.0100	0.1051	0	0.0006	0	0.0056	0.0005	0.0055
c.607G>A	p.Gly203Ser	130 (African)	yes	1.24*	0.0100	0.1061	0	0.0006	0	0.0056	0.0005	0.0055
c.679A>G	p.Ile227Val	130 (African)	yes	1.07	0.0024	0.0267	0	<0.0001	0	0.0006	<0.0001	0.0011
c.844T>G	p.Tyr282Asp	627	n.d.	0.96	0.0087	0.0015	0.0002	0.0125	0.0106	0.0063	0.0031	0.0121
c.943A>G	p.Asn315Asp	386	n.d.	1.25*	0.0035	0.0012	0	0.0040	0.0009	0.0022	0.0068	0.0033
c.1181A>C	p.Tyr394Ser	W17, 121, 288, 289, 999	yes (W17, 121, 999)	2.38**	0.0006	0	0	0.0010	0	0	0	0
c.751C>G	p.Gln251Glu	252, 786	n.d.	1.20*	0	0	0	0	0	0	0	0
c.1136T>A	p.Leu379Gln	252, 786	n.d.	3.34**	0	0	0	0	0	0	0	0
c.1144G>A	p.Val382Met[e]	not applicable	not applicable	2.06**	<0.0001	0	0	<0.0001	0	0	0.0003	0

[a]GenBank: NM_004752.3.
[b]Kindred 130 was of African ancestry and the rest of kindreds were of European ancestry.
[c]Fold over wild-type. *$p < 0.05$, ** $p < 0.01$. n.d., not determined. Data from GBS-luciferase assay in current study.
[d]Approximate total allele numbers in ancestry populations (ExAC browser release 0.3.1): All, n = 121,000; African, n =10,400; East Asian, n = 8,600; non-Finnish European, n = 66,700; Finnish, n = 6,600; Latino, n = 11,500; South Asian, n = 16,500; other, n = 900.
[e]Substitution found in a parathyroid adenoma sample in Mannstadt et al.[15]

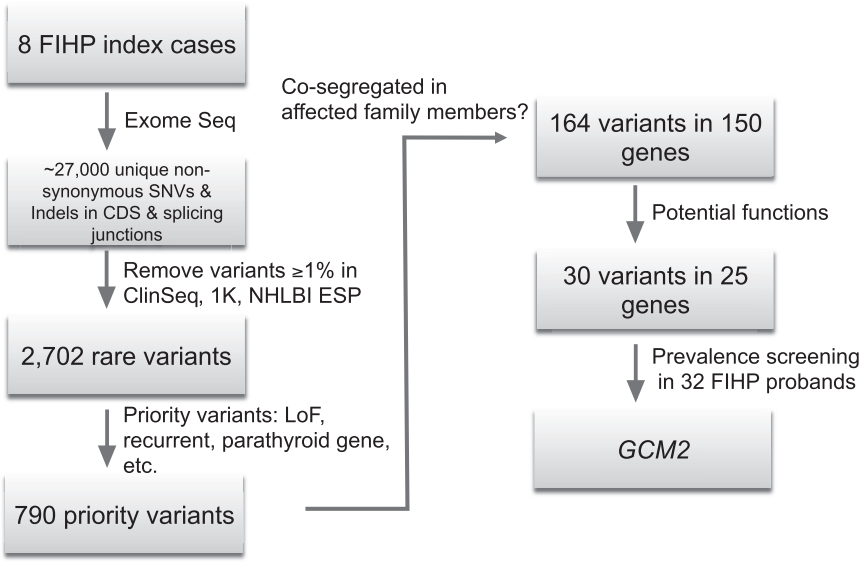

Figure 1. Flowchart of Exome Analysis and Prevalence Screening in Familial Isolated Hyperparathyroidism
SNVs, single-nucleotide variants; indels, insertions or deletions; CDS, coding sequence; LoF, predicted loss-of-function variants; 1K, 1000 Genomes Project; NHLBI ESP, NHLBI GO Exome Sequencing Project.

Q5 high-fidelity Taq, Quick-ligation kit, and PNK (NEB) were used for cloning and mutagenesis. The *GCM2* luciferase reporter construct pGL4-6xGBS-Luc was made by two rounds of cloning of the oligos with three consecutive copies of the GCM-binding site (GBS) 5′-ATGCGGGT-3′ into the pGL4.23[Luc2/minP] vector (Promega). The same GBS was previously used in luciferase reporter assays to study GCM2 activity.[17–20] All plasmid constructs were verified by Sanger sequencing. PCR and cloning oligos are listed in Table S3.

Luciferase Assay

The human embryonic kidney HEK293FT cells (Invitrogen) were cultured in high glucose DMEM (GIBCO) supplemented with 10% fetal bovine serum (Gemini) and penicillin-streptomycin (GIBCO) in an incubator with 5% CO_2. Transfection was performed in suspension with Lipofectamine 2000 (Invitrogen) in 24-well plates. In each well, 400,000 HEK293FT cells were transfected with 375 ng of pGL4-6xGBS-Luc reporter plasmid together with 25 ng of the empty vector or GCM2 expression constructs. Cell lysates were prepared in 1× passive lysis buffer for luciferase assay, 22–24 hr after transfection (Promega). Luciferase activity was measured with a luminometer (Berthold Technologies, Lumat LB 9507). All transfections were performed together in triplicate in at least three independent experiments, and the mean ratios of luciferase activity of *GCM2* constructs to empty vector from three independent experiments were plotted.

Western Blot

To determine the amounts of GCM2 and its mutants, 6 μL of luciferase lysates from an equal-volume mixture of the triplicate experiment was used for SDS-PAGE, followed by western blot. The anti-FLAG M2 (Sigma, no. 3165), anti-GAPDH (Santa Cruz Biotechnology, no. sc-47724) and goat anti-mouse IgG-HRP (Santa Cruz Biotechnology, no. sc-2055) antibodies were used as in standard western blot procedures. After applying the West Pico Chemiluminescent Substrate (Thermo Scientific, no. 34080), polyvinylidene fluoride membranes were imaged with the ChemiDocMP imager (Bio-Rad). Membranes were stripped for re-probing with the OneMinute Plus Western Blot Stripping Buffer (GM Biosciences).

Statistics

Candidate genes of interest with rare variants (n = 30) identified from the FIHP exome cohort (n = 8) were screened in additional probands in the prevalence-screening (validation) cohort (n = 32). We applied Fisher's exact test in a contingency table by using allele frequencies from the 32 FIHP-affected probands and allele frequencies from an ancestry-matched population in the NHLBI ESP6500. Two-tailed p values <0.0017 ($= 0.05/30$) were considered significant. The statistical test used for the luciferase assays was the paired Student's t test (two-tailed), and $p < 0.05$ was considered significant. Two-tailed Mann-Whitney test was used to compare groups with and without C-terminal conserved inhibitory domain (CCID) mutations in *GCM2*. Statistical analyses were performed with Graphpad Prism 5.0 software.

Graphic Illustration

Pedigrees were made with the Madeline 2.0 Pedigree Drawing Engine. The GCM2 protein domain diagram was made with the Illustrator for Biological Sequences (IBS) software. [21]

Results

Exome Analyses of FIHP-Affected Kindreds

We evaluated 40 apparently unrelated kindreds with FIHP (37 with European ancestry, 2 with African ancestry, and 1 with mixed ancestry; Table S2) and selected eight index-case individuals from eight kindreds with FIHP for exome sequencing of blood DNA (Table S2 and Figure S1). Using our established exome sequencing and bioinformatics pipeline,[12] we called and annotated single-nucleotide variants (SNVs) and small insertions or deletions (indels), resulting in ~27,000 unique SNVs and small indels in coding regions or splicing junctions in these eight index-case individuals with FIHP (Figure 1). We focused our analyses on 2,702 rare variants in 2,296 genes with a MAF of less than 1% that were found in three independent projects (ClinSeq, 1000 Genomes, and NHLBI ESP). We then prioritized 790 (29%) rare variants for co-segregation analysis in family members on the basis of the following criteria: if they were recurrent, predicted loss of function (frameshift, nonsense, or in splicing regions), belonged to genes with rare variants in more than one of eight exomes sequenced, or were among genes implicated in parathyroid disease or development. 21% of the prioritized rare variants (164 of 790)

co-segregated with the disease within six of the eight exome-sequenced families available for this testing (Table S4).

Screening for Candidate Variants in the 32 Prevalence-Cohort Kindreds

The 164 rare variants that co-segregated with the disease were present in 150 genes; of these, we selected 30 rare variants in 25 genes of interest for prevalence testing in an additional 32 probands on the basis of potential gene and variant functions (Table S5). 25 of these 30 variants were absent in the prevalence-screening cohort, and therefore they were most likely private rare variants unrelated to FIHP or rare variants of low prevalence in FIHP. The remaining five rare variants were found in one to four additional index-case individuals; of these, the *GCM2* (also known as *GCMB*) variant c.1181A>C (p.Tyr394Ser) in exon 5 was significantly enriched ($n = 4$) ($p < 0.0001$) in the 32 FIHP-affected kindreds in the prevalence cohort, as compared to the ancestry-matched NHLBI ESP6500 population (Fisher's exact test; Bonferroni-corrected p value threshold = 0.0017) (Table S5). Combining the data from the exome and the prevalence cohorts, we found five kindreds with the p.Tyr394Ser variant in affected members.

GCM2 Variants in FIHP-Affected Kindreds

In the prevalence screen, we found two additional probands who showed a rare variant c.1136T>A (p.Leu379Gln) in *GCM2* when a portion of exon 5 was PCR amplified and analyzed by Sanger sequencing. Thus, 7 of 40 FIHP-affected index-case indiviuduals showed recurrent rare variants in *GCM2* in part of exon 5. We then analyzed the entire coding region and intron-exon junctions of *GCM2* in all of the index-case individuals in the 40 FIHP-affected kindreds. We found five more missense variants, one synonymous variant, and one SNV in the 5′ UTR of *GCM2* (Table 1). All *GCM2* variants identified in these samples were heterozygous. No intronic variant was found within 10 bp of a splice site. Three missense variants, c.607G>A (p.Gly203Ser), c.679A>G (p.Ile227Val), and c.844T>G (p.Tyr282Asp), were common in their ancestry-matched populations in the ExAC database (Tables 1 and S2). In contrast, variants c.943A>G (p.Asn315Asp), c.1181A>C (p.Tyr394Ser), c.751C>G (p.Gln251Glu), and c.1136T>A (p.Leu379Gln) were rare variants with MAFs of 0.004, 0.001, 0, and 0, respectively, in the non-Finnish European ancestry population (Tables 1 and S2).

The heterozygous c.751C>G (p.Gln251Glu) and c.1136T>A (p.Leu379Gln) variants were found together in two probands. To determine whether they were present on the same allele, we amplified this region of exon 5 from these two probands and subcloned it into an expression plasmid. Both variants were found in the same plasmid clones, confirming that they were on the same allele. The haplotype with the *cis* variant c.[751C>G; 1136T>A] (p.[Gln251Glu; Leu379Gln]) from these two apparently unrelated kindreds likely shares a common ancestor given that these two variants and another variant in *GCM2* intron 3 (c.456+16A>C) found in these two probands were absent in ~120,000 alleles in the ExAC database.

A co-segregation test in kindreds for which DNA was available from additional members showed that the p.Tyr394Ser variant co-segregated in four of four affected members in kindred W17, two of two affected members in kindred 121, and two of two affected members in kindred 999 (Figure 2). The individual II-4 in kindred W17 (Figure 2A) with no consanguinity reported was homozygous for this variant. Both of the p.Gly203Ser and p.Ile227Val variants were associated with PHPT in kindred 130. DNA samples from other affected members were unavailable for co-segregation testing in the other six kindreds shown in Figure 2.

A fresh frozen parathyroid tumor sample was available from one individual (proband in kindred 999) with the heterozygous p.Tyr394Ser variant. Sanger sequencing of the cDNA sample prepared from the tumor showed that both the variant and wild-type alleles were expressed in the tumor (Figure S2).

Prevalence screening and co-segregation analysis thus supported that *GCM2* was the most prevalent gene harboring rare variants in FIHP in our analyses; three rare variant alleles, c.943A>G (p.Asn315Asp), c.1181A>C (p.Tyr394Ser), and c.[751C>G; 1136T>A] (p.[Gln251Glu; Leu379Gln]), were found in 8 of 40 (20%) FIHP-affected kindreds analyzed.

Functional Analyses of *GCM2* Variants

GCM2 encodes a transcription factor whose expression is largely restricted to the parathyroid gland. It is required for parathyroid development during embryogenesis, given that *Gcm2* knockout mice lack parathyroid glands.[22] Previously, several frameshift, nonsense, and missense mutations of *GCM2* were reported in families with isolated hypoparathyroidism (Table S6). These mutants were shown to possess lower transcriptional activity than wild-type GCM2 in functional assays in which three or six copies of a consensus GBS arranged in tandem were located upstream of a luciferase reporter. Using a luciferase reporter with six copies of GBS, we tested whether the *GCM2* variants found in our FIHP-affected kindreds affected the transcription-activating function of GCM2.

In HEK293FT cells, wild-type GCM2 activated the GBS luciferase reporter 5-fold as compared to the empty vector control (Figure 3A). GCM2 variants p.Leu379Gln, p.[Gln251Glu; Leu379Gln], and p.Tyr394Ser activated the GBS luciferase reporter 16-, 18-, and 11-fold, respectively, over the empty vector control, representing 3.3, 3.7, and 2.4 times higher activity, respectively, than wild-type GCM2. Variants p.Gly203Ser, p.Asn315Asp, and p.Gln251Glu showed only 20% higher activity than the wild-type; however, the differences between them and the wild-type were statistically significant ($p < 0.05$). In contrast, variants p.Ile227Val and p.Tyr282Asp displayed activity similar to that of the wild-type GCM2.

In addition to these *GCM2* variants found in the individuals with FIHP, we also tested the transactivating function

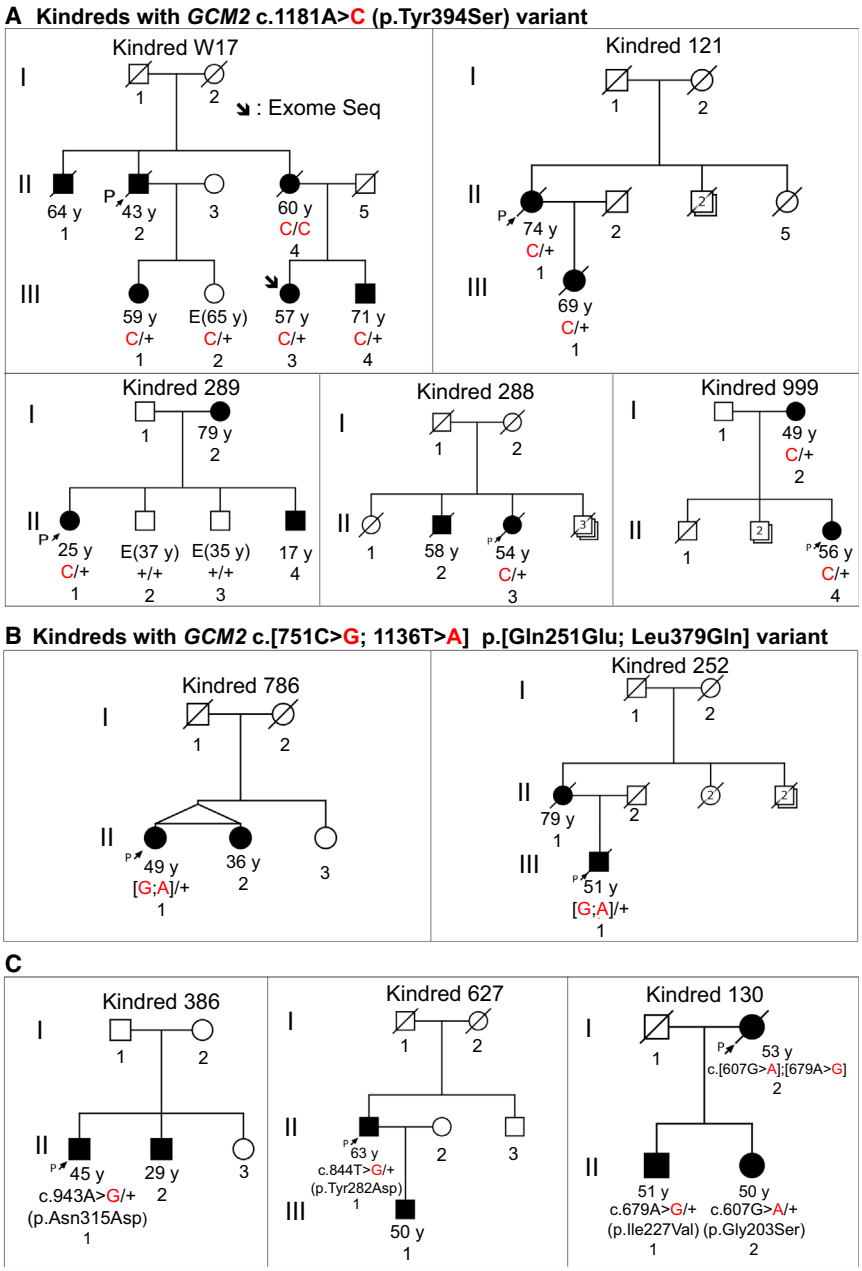

Figure 2. Pedigrees of Familial Isolated Hyperparathyroidism Kindreds with *GCM2* Variants

(A–C) The pedigrees of kindreds with individuals harboring c.1181A>C (p.Tyr394Ser) (A), c.[751C>G; 1136T>A] (p.[Gln251Glu; Leu379Gln]) (B), and other (C) variants. Black-filled symbols represent individuals diagnosed with PHPT. Open symbols represent individuals with unavailable calcium levels, except those specifically noted (denoted by E) in the pedigree. *GCM2* genotypes are shown for all individuals with available germline DNA. Numbers followed by the unit "y" (years) under boxes (male) or circles (female) denote age at diagnosis of PHPT. In kindred 786, identical twins are indicated by a horizontal line connecting the diagonal lines. Slash, deceased; smaller thin arrow, probands (P); larger thick arrow, sample subjected to exome sequencing (in kindred W17); +, wild-type allele; E, normal calcium and PTH levels when evaluated at the indicated age.

of a mutation or polymorphism previously reported in a sporadic parathyroid adenoma sample, c.1144G>A (p.Val382Met).[15] p.Val382Met activated the GBS luciferase reporter 10-fold, which corresponds to 2.1 times higher activity than wild-type GCM2.

The steady-state levels of the transfected GCM2 were similar (Figure 3B), suggesting that the increased transcriptional activities of GCM2 variants were due to enhanced transactivating function.

Characterization of the Transcription Inhibitory Domain of GCM2

Previously, via chimeric constructs of the C terminus of mouse GCM2 and the DNA binding domain from another transcription factor, the mouse GCM2 C terminus was shown to contain two transactivation domains encompassing amino acids (aa) 175–263 and 426–504 and an inhibitory region encompassing aa 264–352 (Figure 3C).[23] The region (aa 353–425) located between the inhibitory region and the C-terminal transactivation domain was non-annotated.[23] Because three GCM2 variants (p.Leu379Gln, p.Val382Met, and p.Tyr394Ser) with the strongest transactivation function were located within the non-annotated highly conserved region (Figure 3D), we characterized the role of the region between the two transactivation domains in the context of human GCM2. We made a series of deletion constructs and tested their transactivating function in GBS-luciferase-reporter assays (Figure 3E). Surprisingly, deletion of the previously annotated inhibitory region (aa 264–352) did not enhance transactivation significantly. In contrast, the deletion of aa 343–427 enhanced transactivation 6-fold as compared to the wild-type. The construct with aa 264–427 deletion displayed markedly lower transactivation than that from the deletion of aa 343–427, suggesting that the region between aa 264 and 342 is required for optimum transactivating function of GCM2. More impressively, deletion of a 20 aa region (Δ377–396) containing leucine 379, valine 382 and tyrosine 394 increased transactivation 8-fold over that of the wild-type (Figure 3E). The protein steady-state level of the Δ377–396 construct was 40% higher than that of wild-type GCM2 (Figure 3F), indicating that this 20 aa region harbors a strong

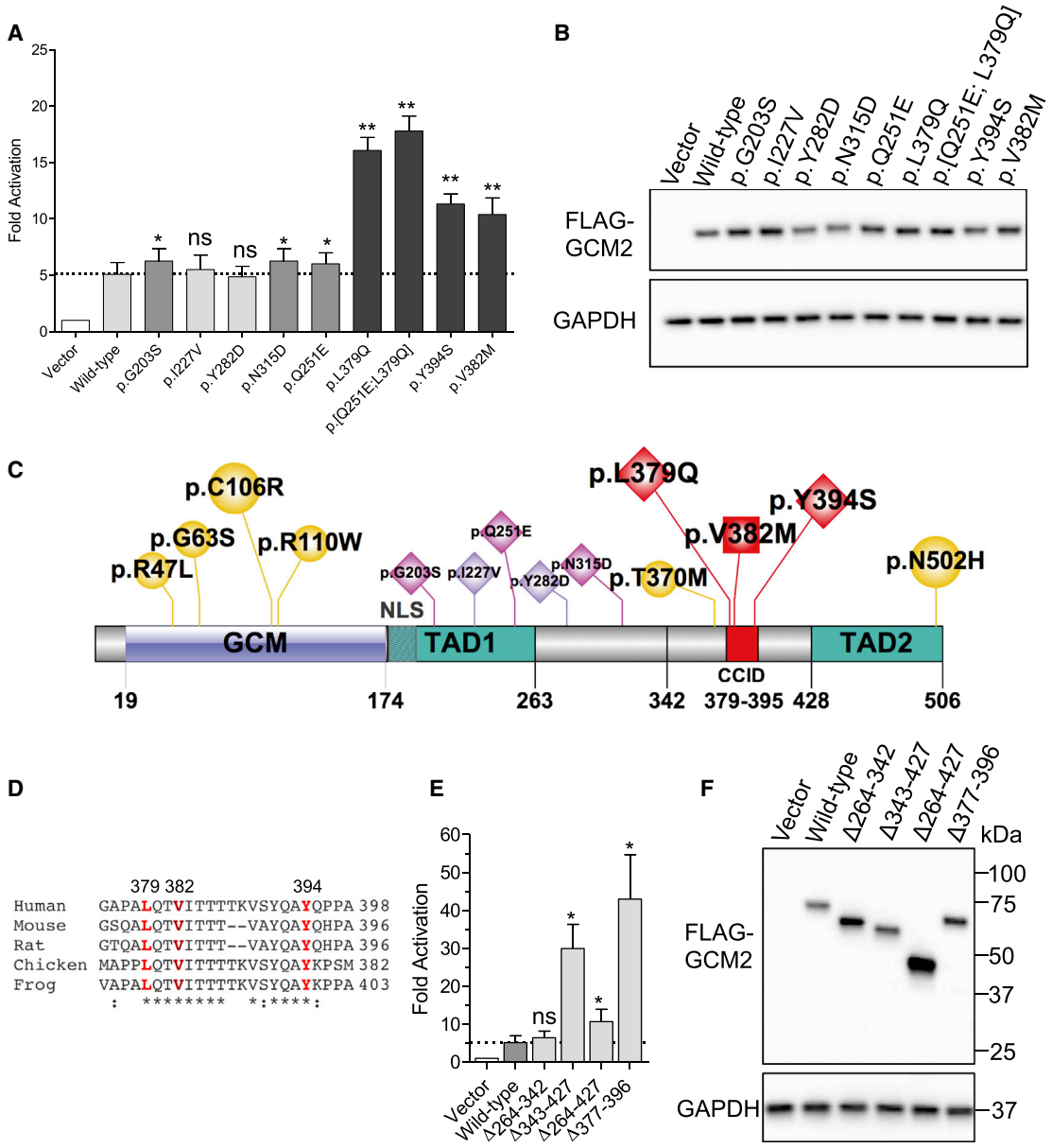

Figure 3. GCM2 Variants and Protein Domains

(A) Luciferase assays for wild-type GCM2 and variants found in FIHP-affected kindreds. 25 ng of empty vector, wild-type GCM2, or the indicated GCM2 variants were co-transfected with 375 ng of 6xGBS luciferase reporter plasmid in HEK293FT cells. The ratios of luciferase activities of GCM2 constructs over empty vectors were plotted. Each sample was transfected in triplicate, and the means of three independent experiments are shown. Error bars denote SEM. p values of paired two-tailed t test were used for comparisons between variants and wild-type GCM2. ns, not significant. *$p < 0.05$, **$p < 0.01$.

(B) Representative western blots of one of the experiments shown in (A). An equal volume of luciferase lysates was analyzed with anti-FLAG to detect transfected GCM2. GAPDH was used as the loading control.

(C) GCM2 protein domains. Transactivating domains 1 and 2 have been characterized in Tuerk et al.[23] CCID, C-terminal conserved inhibitory domain. TAD, transactivating domain. NLS, nuclear localization signal. Yellow circles, germline missense mutations reported in individuals with hypoparathyroidism; square, p.Val382Met substitution found in a parathyroid adenoma sample in Mannstadt et al.;[15] rhombuses, mutations found in the germline of FIHP-mutation kindreds in our study. Light purple, pink, and red colors of the rhombus-shaped mutations indicate their similar, slightly elevated, and markedly increased transactivating activities, respectively, as compared to wild-type.

(D) Alignment of GCM2 at the CCID. Figure S3 shows full protein alignment.

(E and F) Luciferase assays (E) and western blots (F) of GCM2 deletion constructs, performed as in panels (A) and (B).

transcriptional inhibitory signal and might also modestly diminish the amount of GCM2.

Although the N-terminal GCM domain of the GCM family of proteins is conserved from *Drosophila* to human,[24] most of the C termini of GCM2 homologs in vertebrates with parathyroid glands are divergent (Figure S3). However, the aa 379–395 region is the only conserved region apart from the N-terminal GCM domain (Figure S3).

Therefore, we named the region encompassing aa 379–395 as the CCID of GCM2.

Together, the genetic evidence and functional assays demonstrates that *GCM2* mutations leading to amino acid changes in the CCID, p.[Gln251Glu; Leu379Gln] and p.Tyr394Ser, are pathologic transcription-activating mutations that can cause FIHP. This mutational consequence contrasts with the inactivating properties of *GCM2* mutations that cause familial hypoparathyroidism.

Mutation Analyses of *GCM2* Region Encoding CCID in Sporadic Parathyroid Adenoma Tissues

We sequenced the region encoding the CCID in *GCM2* in two cohorts of parathyroid tumor samples from individuals with sporadic PHPT. No *GCM2* CCID variant was found in the 87 parathyroid tumor DNA samples, which have matched germline DNA available. In another set of 20 cDNA samples prepared from de-identified parathyroid tumors without germline DNA available, we found one sample with the p.Tyr394Ser substitution. Thus, germline or somatic *GCM2* CCID variants in sporadic cases are uncommon.

Phenotype of Individuals with *GCM2* Variations

In the seven FIHP-affected kindreds with *GCM2* CCID variants p.[Gln251Glu; Leu379Gln] and p.Tyr394Ser, there were 19 individuals (13 females and 6 males) with PHPT, and one carrier (individual III-2 in kindred W17, Figure 2A). Five of seven kindreds had only two hypercalcemic members. These people were diagnosed at 17 to 79 years of age (median, 57 years old) (Table S2). These two mutations were associated with multiple parathyroid tumors in 14 of 17 (82%) operations of evaluable cases (Table S2). The proband in kindred W17 was the only individual who might have had parathyroid cancer[25] in these seven kindreds. The individual II-4, with a homozygous *GCM2* p.Tyr394Ser variant, in kindred W17 (Figure 2A) did not display unusual or more severe symptoms as compared to other people with PHPT and carrying the heterozygous mutation.

Four of 19 individuals with PHPT had kidney stones or nephrolithiasis, and three additional persons had osteopenia. Individuals with *GCM2* CCID mutations did not have a recurring pattern of non-parathyroid neoplasms diagnosed at the time of diagnosis of PHPT or during follow-up; three individuals in kindreds 121 and 252 had ovarian, pancreatic, colorectal, or breast cancer (Table S2).

To determine whether *GCM2* CCID mutations confer characteristic features among individuals with FIHP, we compared several parameters among the *GCM2* CCID mutant group (seven probands) and the *GCM2* wild-type group (30 probands) and found that the maximum dimensions of the largest parathyroid glands resected were not only large but also significantly larger in the *GCM2* CCID mutant group than in the wild-type FIHP group (median, 3 cm versus 2 cm; $p = 0.03$, Mann-Whitney test) (Figure S4).

Discussion

Four main genes were previously identified as being mutated in five distinct familial syndromes with PHPT (*MEN1*, *RET*, *CASR* [causing two types of syndromes], and *CDC73*); rarer germline mutations in other genes (*CDKN1A* [MIM: 116899], *CDKN1B* [MIM: 600778], *CDKN2B* [MIM: 600431], *CDKN2C* [MIM: 603369], *AP2S1* [MIM: 602242], *GNA11* [MIM: 139313], and *SLC12A1* [MIM: 600839]) also contribute to familial PHPT, but no gene specific for FIHP has been identified (Table S1).[26–31] We studied 40 FIHP-affected kindreds with no mutations found in *MEN1*, *CASR,* or *CDC73*. We found two recurrent rare *GCM2* variants (p.[Gln251Glu; Leu379Gln] and p.Tyr394Ser) in seven (18%) of 40 FIHP-affected kindreds and one rare variant (p.Asn315Asp) in one FIHP-affected kindred (Table 1). The substantial fraction (82%) of our FIHP-affected kindreds without a *GCM2* CCID mutation suggests genetic or other heterogeneity in FIHP cases. Other mechanisms activating GCM2, or those unrelated to GCM2 in kindreds without a *GCM2* CCID mutation, might have caused the similar phenotypes seen among the two groups with and without CCID mutations (Figure S4).

One limitation of this study is that only 29% of rare variants in protein coding regions were characterized in detail, and therefore other candidate genes and variants in non-coding regions might have been missed. It is also possible that cases of FIHP in some of our 40 kindreds might represent phenocopies rather than being caused by germline mutations, in particular, in the kindreds with only two known affected members. An occult syndromal case might not have been recognized for lack of mutation in DNA screening.

GCM2, located on human chromosome 6p24.2, encodes a 506 aa transcription factor. In *Drosophila*, the prototype glial cells missing (*gcm*) controls the fate decision between glial and neuronal lineages.[32] In mammals, *GCM2* is mainly expressed in the parathyroid glands and its expression persists into adulthood, and low-level *GCM2* expression is also observed in the brain during development.[33,34] GCM2 is a master regulator of parathyroid gland development; mice with conventional or conditional loss of *Gcm2* lack parathyroid glands, and germline mutations that inactivate *GCM2* can cause hypoparathyroidism (Table S6).[22,35–37] Most likely, one of the functions of GCM2 in parathyroid cells is to activate PTH transcription in cooperation with other transcription factors such as GATA3 and MAFB, given that the PTH promoter contains a consensus GCM-binding site and GCM2 is capable of activating PTH promoter in reporter assays.[38,39] Given the highly restricted expression pattern of *GCM2*, *GCM2*-activating mutations are not likely to cause the non-parathyroid traits

commonly seen in individuals with MEN1 or HPT-JT syndromes. Expectations of cure by parathyroidectomy and relief from the burden of uncertainty of developing other tumors will likely improve the quality of life for people with *GCM2*-activating mutations.

Our genetic data and *GCM2* transcriptional assays provide solid support for the *GCM2* CCID variants studied here as pathologic activating mutations. First, the activation pattern was essentially the inverse of that observed in familial hypoparathyroidism, as reported previously; second, a small critical protein domain (CCID) was highlighted in both genetic screening and deletion analyses; third, CCID was selectively conserved across species among tetrapods. Thus, *GCM2* mutations can cause hypo- or hyper-parathyroidism. This is analogous to inactivating or activating mutations in several other genes, which evoke a wide spectrum of function from abnormally high to abnormally low in some processes. This includes genes regulating insulin (*ABCC8* [MIM: 600509], *GCK* [MIM: 138079], *INSR* [MIM: 147670], and *KCNJ11* [MIM: 600937]), thyroxine, (*TSHR* [MIM: 603372]), and testosterone (*LHR* [MIM: 152790]), as well as two other genes that regulate PTH (*CASR* [MIM: 601199] and *GNA11* [MIM: 139313]). GCM2 is a possible target for pharmacologic manipulation of PTH excess or deficiency.

Of the three CCID variants we characterized, the p.Leu379Gln variant was not found in the general population, containing ~120,000 alleles, in the ExAC database. The p.Tyr394Ser variant is relatively more common in non-Finnish Europeans, with a prevalence of 0.20%, but is not found in other populations. The p.Val382Met substitution was previously reported in a sporadic parathyroid adenoma sample, and it is not known whether it was also in the germline.[15] The p.Val382Met variant is present in 0.01% of non-Finnish Europeans and in 0.05% of the South Asian population (Table 1). All the kindreds with p.Tyr394Ser in our study were of European ancestry. Our data, together with the ExAC database, suggest that two *GCM2* CCID variants (p.Tyr394Ser and p.Val382Met) predispose 0.21% of the population of European ancestry and 0.05% of the population of South Asian ancestry to develop PHPT. However, this needs to be cautiously interpreted. The ExAC database (release 0.3.1) contains data from 33,350 non-Finnish Europeans and 8,250 South Asians who were participants in specific disease and human population studies and thus might not represent the true general population. It is also possible that some populations might be over-represented in the ExAC database. Although the numbers of participants in the ExAC database are large, their phenotypes are not available to the public. Therefore, large-scale genetic screening with phenotypic follow-up will be critical to understand the prevalence and penetrance of *GCM2*-activating mutations. The estimates of prevalence of PHPT among adults vary widely, from 0.1% to 9.4%, depending on the calendar year of the estimate, geography, diagnostic criteria, age, gender, and race (Table S7). It will be important to analyze the penetrance of *GCM2* CCID variants in PHPT among different age and gender groups.

The remaining five *GCM2* variants found in FIHP-affected kindreds were not located in the GCM2 CCID. These variants showed modestly increased transactivation (p.Gly203Ser, p.Asn315Asp, and p.Gln251Glu) or normal transcriptional activity (p.Ile227Val and p.Tyr282Asp). Recently, the allele frequencies of p.Tyr282Asp were found to be 6.5% among three large Italian cohorts with sporadic PHPT and 2.9% among controls.[40] In that study, the p.Tyr282Asp variant showed a modest 1.4-fold increase in transcriptional activity.[40] Such variants located outside the CCID are relatively more common, particularly in certain populations (Table 1). The modestly increased transactivation of p.Gly203Ser, p.Asn315Asp, and p.Gln251Glu suggests that they could contribute to PHPT; however, variants p.Gly203Ser and p.Asn315Asp, as well as p.Ile227Val and p.Tyr282Asp, were not enriched in kindreds with FIHP as compared to ancestry-matched general populations, providing a strong piece of genetic evidence against their involvement in PHPT. Therefore, we consider these variants located outside of GCM2 CCID unlikely to be pathologic activating mutations. However, it is possible that these variants could contribute subtly to PHPT. Studies with large-scale genotype-phenotype association in various populations, studies in animal models, or other assays could help delineate the functions of these variants.

Our results point to the possibility that *GCM2* might also be involved in the pathogenesis of sporadic parathyroid adenomas. Interestingly, we found that the p.Val382Met variant, which was reported in a parathyroid adenoma,[15] also showed increased transcriptional activity. Note that this variant was previously shown not to affect the transcriptional activity of GCM2 in the chicken DF-1 fibroblast cell line.[15] HEK293FT cells are epithelial cells, and perhaps a better model for GCM2 functional analysis than a fibroblast cell line. Our data and the fact that p.Val382Met was found in an adenoma sample suggest that it could be associated with PHPT by acting as a gain-of-function mutation. Previously, it was reported that one adenoma sample out of 30 contained a *GCM2* mutation or polymorphism.[15] We found one adenoma sample with a GCM2 CCID variant (p.Tyr394Ser) among 107 parathyroid adenomas analyzed. Therefore, *GCM2*-activating mutations contribute to only a small percentage of sporadic adenoma cases when tested mainly among postmenopausal women. Other mechanisms, such as increased mRNA expression or enhanced protein activity of GCM2, might be critical for parathyroid adenoma development. In fact, it has been shown that GCM2 was overexpressed in 47% of parathyroid adenomas, although another study reported that GCM2 was not overexpressed in adenomas.[41,42]

Our results support a central role of *GCM2* in PHPT. As a corollary, this study proves that FIHP can be caused by germline mutation of a non-syndromal gene. Because the mutations are activating and associated with parathyroid

tumors and PHPT, we tentatively consider *GCM2* as a parathyroid proto-oncogene, analogous to *RET* in the parathyroid tissues of MEN2A. Our data, along with human genome survey data in the ExAC database, suggest that *GCM2*-activating mutations could be one of the most common causes of familial hyperparathyroidism. Our findings of *GCM2*-activating mutations in FIHP are expected to have an important impact on clinical practice, including treatment decisions and genetic testing of individuals with PHPT and their family members.

Supplemental Data

Supplemental Data include four figures and seven tables and can be found with this article online at http://dx.doi.org/10.1016/j.ajhg.2016.08.018.

Acknowledgments

The authors are grateful to the participants in this study. We thank members at the National Institute of Diabetes and Digestive and Kidney Diseases (NIDDK) Clinical Laboratory Core for storage of DNA samples. We would like to thank Mr. Craig Cochran and the NIH 5NW nursing staff for their expert patient care. We also thank our colleagues Drs. Lee Weinstein, Monica Skarulis, and Michael Collins, as well as the past and present fellows of the National Institute of Child Health and Human Development (NICHD)-NIDDK Interinstitute Endocrine Training Program. This work was supported by the Intramural Research Program of the NIH, the NIDDK (S.J.M., S.K.A., and W.F.S.), the National Human Genome Research Institute (L.G.B., J.C.S., and J.J.J.), the Eunice Kennedy Shriver National Institute of Child Health and Human Development (S.J.M.), and the National Cancer Institute (E.K.).

Received: June 29, 2016
Accepted: August 29, 2016
Published: October 13, 2016

Web Resources

CLINSEQ, https://www.genome.gov/20519355
ExAC Browser, http://exac.broadinstitute.org/
GenBank, http://www.ncbi.nlm.nih.gov/genbank/
Madeline 2.0 Pedigree Drawing Engine, https://madeline.med.umich.edu/madeline/index.php
NCBI Genome, http://www.ncbi.nlm.nih.gov/genome/
OMIM, http://www.omim.org/

References

1. Marcocci, C., and Cetani, F. (2011). Clinical practice. Primary hyperparathyroidism. N. Engl. J. Med. *365*, 2389–2397.
2. Silverberg, S.J., and Bilezikian, J.P. (2006). The diagnosis and management of asymptomatic primary hyperparathyroidism. Nat. Clin. Pract. Endocrinol. Metab. *2*, 494–503.
3. Hendy, G.N., and Cole, D.E. (2013). Genetic defects associated with familial and sporadic hyperparathyroidism. Front. Horm. Res. *41*, 149–165.
4. Hannan, F.M., Nesbit, M.A., Christie, P.T., Fratter, C., Dudley, N.E., Sadler, G.P., and Thakker, R.V. (2008). Familial isolated primary hyperparathyroidism caused by mutations of the MEN1 gene. Nat. Clin. Pract. Endocrinol. Metab. *4*, 53–58.
5. Marcocci, C., Bollerslev, J., Khan, A.A., and Shoback, D.M. (2014). Medical management of primary hyperparathyroidism: proceedings of the fourth International Workshop on the Management of Asymptomatic Primary Hyperparathyroidism. J. Clin. Endocrinol. Metab. *99*, 3607–3618.
6. Starker, L.F., Akerström, T., Long, W.D., Delgado-Verdugo, A., Donovan, P., Udelsman, R., Lifton, R.P., and Carling, T. (2012). Frequent germ-line mutations of the MEN1, CASR, and HRPT2/CDC73 genes in young patients with clinically non-familial primary hyperparathyroidism. Horm. Cancer *3*, 44–51.
7. Iacobone, M., Carnaille, B., Palazzo, F.F., and Vriens, M. (2015). Hereditary hyperparathyroidism–a consensus report of the European Society of Endocrine Surgeons (ESES). Langenbecks Arch. Surg. *400*, 867–886.
8. Li, Y., and Simonds, W.F. (2016). Endocrine neoplasms in familial syndromes of hyperparathyroidism. Endocr. Relat. Cancer *23*, R229–R247.
9. Simonds, W.F., James-Newton, L.A., Agarwal, S.K., Yang, B., Skarulis, M.C., Hendy, G.N., and Marx, S.J. (2002). Familial isolated hyperparathyroidism: clinical and genetic characteristics of 36 kindreds. Medicine (Baltimore) *81*, 1–26.
10. Simonds, W.F., Robbins, C.M., Agarwal, S.K., Hendy, G.N., Carpten, J.D., and Marx, S.J. (2004). Familial isolated hyperparathyroidism is rarely caused by germline mutation in HRPT2, the gene for the hyperparathyroidism-jaw tumor syndrome. J. Clin. Endocrinol. Metab. *89*, 96–102.
11. Warner, J., Epstein, M., Sweet, A., Singh, D., Burgess, J., Stranks, S., Hill, P., Perry-Keene, D., Learoyd, D., Robinson, B., et al. (2004). Genetic testing in familial isolated hyperparathyroidism: unexpected results and their implications. J. Med. Genet. *41*, 155–160.
12. Johnston, J.J., Sanchez-Contreras, M.Y., Keppler-Noreuil, K.M., Sapp, J., Crenshaw, M., Finch, N.A., Cormier-Daire, V., Rademakers, R., Sybert, V.P., and Biesecker, L.G. (2015). A Point Mutation in PDGFRB Causes Autosomal-Dominant Penttinen Syndrome. Am. J. Hum. Genet. *97*, 465–474.
13. Parsons, D.W., Li, M., Zhang, X., Jones, S., Leary, R.J., Lin, J.C., Boca, S.M., Carter, H., Samayoa, J., Bettegowda, C., et al. (2011). The genetic landscape of the childhood cancer medulloblastoma. Science *331*, 435–439.
14. Jones, S., Li, M., Parsons, D.W., Zhang, X., Wesseling, J., Kristel, P., Schmidt, M.K., Markowitz, S., Yan, H., Bigner, D., et al. (2012). Somatic mutations in the chromatin remodeling gene ARID1A occur in several tumor types. Hum. Mutat. *33*, 100–103.
15. Mannstadt, M., Holick, E., Zhao, W., and Jüppner, H. (2011). Mutational analysis of GCMB, a parathyroid-specific transcription factor, in parathyroid adenoma of primary hyperparathyroidism. J. Endocrinol. *210*, 165–171.
16. Adereth, Y., Champion, K.J., Hsu, T., and Dammai, V. (2005). Site-directed mutagenesis using Pfu DNA polymerase and T4 DNA ligase. Biotechniques *38*, 864–868.
17. Mirczuk, S.M., Bowl, M.R., Nesbit, M.A., Cranston, T., Fratter, C., Allgrove, J., Brain, C., and Thakker, R.V. (2010). A missense glial cells missing homolog B (GCMB) mutation, Asn502His, causes autosomal dominant hypoparathyroidism. J. Clin. Endocrinol. Metab. *95*, 3512–3516.

18. Mannstadt, M., Bertrand, G., Muresan, M., Weryha, G., Leheup, B., Pulusani, S.R., Grandchamp, B., Jüppner, H., and Silve, C. (2008). Dominant-negative GCMB mutations cause an autosomal dominant form of hypoparathyroidism. J. Clin. Endocrinol. Metab. *93*, 3568–3576.
19. Thomée, C., Schubert, S.W., Parma, J., Lê, P.Q., Hashemolhosseini, S., Wegner, M., and Abramowicz, M.J. (2005). GCMB mutation in familial isolated hypoparathyroidism with residual secretion of parathyroid hormone. J. Clin. Endocrinol. Metab. *90*, 2487–2492.
20. Schreiber, J., Sock, E., and Wegner, M. (1997). The regulator of early gliogenesis glial cells missing is a transcription factor with a novel type of DNA-binding domain. Proc. Natl. Acad. Sci. USA *94*, 4739–4744.
21. Liu, W., Xie, Y., Ma, J., Luo, X., Nie, P., Zuo, Z., Lahrmann, U., Zhao, Q., Zheng, Y., Zhao, Y., et al. (2015). IBS: an illustrator for the presentation and visualization of biological sequences. Bioinformatics *31*, 3359–3361.
22. Günther, T., Chen, Z.F., Kim, J., Priemel, M., Rueger, J.M., Amling, M., Moseley, J.M., Martin, T.J., Anderson, D.J., and Karsenty, G. (2000). Genetic ablation of parathyroid glands reveals another source of parathyroid hormone. Nature *406*, 199–203.
23. Tuerk, E.E., Schreiber, J., and Wegner, M. (2000). Protein stability and domain topology determine the transcriptional activity of the mammalian glial cells missing homolog, GCMb. J. Biol. Chem. *275*, 4774–4782.
24. Akiyama, Y., Hosoya, T., Poole, A.M., and Hotta, Y. (1996). The gcm-motif: a novel DNA-binding motif conserved in Drosophila and mammals. Proc. Natl. Acad. Sci. USA *93*, 14912–14916.
25. Mallette, L.E., Bilezikian, J.P., Ketcham, A.S., and Aurbach, G.D. (1974). Parathyroid carcinoma in familial hyperparathyroidism. Am. J. Med. *57*, 642–648.
26. Marx, S.J. (2011). Hyperparathyroid genes: sequences reveal answers and questions. Endocr. Pract. *17* (*Suppl 3*), 18–27.
27. Agarwal, S.K., Mateo, C.M., and Marx, S.J. (2009). Rare germline mutations in cyclin-dependent kinase inhibitor genes in multiple endocrine neoplasia type 1 and related states. J. Clin. Endocrinol. Metab. *94*, 1826–1834.
28. Lee, M., and Pellegata, N.S. (2013). Multiple endocrine neoplasia type 4. Front. Horm. Res. *41*, 63–78.
29. Warner, J.V., Nyholt, D.R., Busfield, F., Epstein, M., Burgess, J., Stranks, S., Hill, P., Perry-Keene, D., Learoyd, D., Robinson, B., et al. (2006). Familial isolated hyperparathyroidism is linked to a 1.7 Mb region on chromosome 2p13.3-14. J. Med. Genet. *43*, e12.
30. Li, D., Tian, L., Hou, C., Kim, C.E., Hakonarson, H., and Levine, M.A. (2016). Association of mutations in SLC12A1 encoding the NKCC2 cotransporter with neonatal primary hyperparathyroidism. J. Clin. Endocrinol. Metab. *101*, 2196–2200.
31. Gross, I., Siedner-Weintraub, Y., Simckes, A., and Gillis, D. (2015). Antenatal Bartter syndrome presenting as hyperparathyroidism with hypercalcemia and hypercalciuria: a case report and review. J. Pediatr. Endocrinol. Metab. *28*, 943–946.
32. Mao, H., Lv, Z., and Ho, M.S. (2012). Gcm proteins function in the developing nervous system. Dev. Biol. *370*, 63–70.
33. Grigorieva, I.V., and Thakker, R.V. (2011). Transcription factors in parathyroid development: lessons from hypoparathyroid disorders. Ann. N Y Acad. Sci. *1237*, 24–38.
34. Kim, J., Jones, B.W., Zock, C., Chen, Z., Wang, H., Goodman, C.S., and Anderson, D.J. (1998). Isolation and characterization of mammalian homologs of the Drosophila gene glial cells missing. Proc. Natl. Acad. Sci. USA *95*, 12364–12369.
35. Ding, C., Buckingham, B., and Levine, M.A. (2001). Familial isolated hypoparathyroidism caused by a mutation in the gene for the transcription factor GCMB. J. Clin. Invest. *108*, 1215–1220.
36. Canaff, L., Zhou, X., Mosesova, I., Cole, D.E., and Hendy, G.N. (2009). Glial cells missing-2 (GCM2) transactivates the calcium-sensing receptor gene: effect of a dominant-negative GCM2 mutant associated with autosomal dominant hypoparathyroidism. Hum. Mutat. *30*, 85–92.
37. Yuan, Z., Opas, E.E., Vrikshajanani, C., Libutti, S.K., and Levine, M.A. (2014). Generation of mice encoding a conditional null allele of Gcm2. Transgenic Res. *23*, 631–641.
38. Kamitani-Kawamoto, A., Hamada, M., Moriguchi, T., Miyai, M., Saji, F., Hatamura, I., Nishikawa, K., Takayanagi, H., Hitoshi, S., Ikenaka, K., et al. (2011). MafB interacts with Gcm2 and regulates parathyroid hormone expression and parathyroid development. J. Bone Miner. Res. *26*, 2463–2472.
39. Han, S.I., Tsunekage, Y., and Kataoka, K. (2015). Gata3 cooperates with Gcm2 and MafB to activate parathyroid hormone gene expression by interacting with SP1. Mol. Cell. Endocrinol. *411*, 113–120.
40. D'Agruma, L., Coco, M., Guarnieri, V., Battista, C., Canaff, L., Salcuni, A.S., Corbetta, S., Cetani, F., Minisola, S., Chiodini, I., et al. (2014). Increased prevalence of the GCM2 polymorphism, Y282D, in primary hyperparathyroidism: analysis of three Italian cohorts. J. Clin. Endocrinol. Metab. *99*, E2794–E2798.
41. Kebebew, E., Peng, M., Wong, M.G., Ginzinger, D., Duh, Q.Y., and Clark, O.H. (2004). GCMB gene, a master regulator of parathyroid gland development, expression, and regulation in hyperparathyroidism. Surgery *136*, 1261–1266.
42. Correa, P., Akerström, G., and Westin, G. (2002). Underexpression of Gcm2, a master regulatory gene of parathyroid gland development, in adenomas of primary hyperparathyroidism. Clin. Endocrinol. (Oxf.) *57*, 501–505.